NANO LETTERS

Letter

pubs.acs.org/NanoLett

Plasmonic Resonant Solitons in Metallic Nanosuspensions

Shima Fardad,[†,‡] Alessandro Salandrino,[§] Matthias Heinrich,[†] Peng Zhang,[‡,§] Zhigang Chen,*[,‡,∥] and Demetrios N. Christodoulides*[,†]

[†]CREOL/College of Optics, University of Central Florida, Orlando, Florida 32816, United States

[‡]Department of Physics and Astronomy, San Francisco State University, San Francisco, California 94132, United States

[§]Currently with NSF Nanoscale Science and Engineering Center, University of California, Berkeley, California 94720, United States

[∥]TEDA Applied Physics Institute and School of Physics, Nankai University, Tianjin 300457, China

ABSTRACT: Robust propagation of self-trapped light over distances exceeding 25 diffraction lengths has been demonstrated for the first time in plasmonic nanosuspensions. This phenomenon results from the interplay between optical forces and enhanced polarizability that would have been otherwise impossible in conventional dielectric dispersions. Plasmonic nanostructures such as core−shell particles, nanorods, and spheres are shown to display tunable polarizabilities depending on their size, shape, and composition, as well as the wavelength of illumination. Here we discuss nonlinear light−matter dynamics arising from an effective positive Kerr effect, which in turn allows for deep penetration of long needles of light through dissipative colloidal media. Our findings may open up new possibilities toward synthesizing soft-matter systems with customized optical nonlinearities.

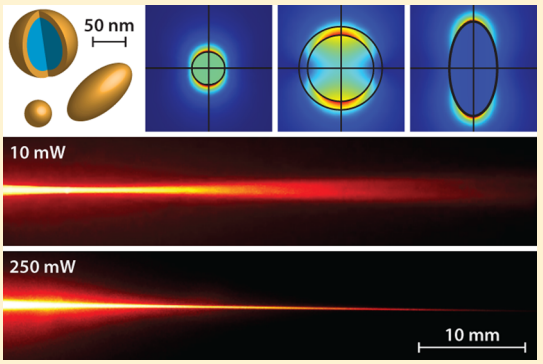

KEYWORDS: *Metallic nanosuspension, plasmonic resonance, core−shell particle, optical self-trapping, Kerr effect, negative polarizability*

In recent years, the development of artificial materials exhibiting novel optical properties has become one of the major scientific endeavors. Of particular interest are soft-matter systems, which play a central role in numerous fields ranging from life sciences to chemistry and physics.[1−5] Yet, despite their broad relevance, managing the dynamics of light in colloidal arrangements still remains problematic. Two primary reasons are known to contribute to this challenge: First, in typical colloids, light−matter interactions are generally dominated by strong scattering effects. Second, the range of optical beam propagation in such media is severely limited as a result of catastrophic self-focusing collapse.[6,7] Evidently, controlling these processes in order to stabilize and extend beam propagation in soft-matter environments could have a significant impact on numerous areas, as for example optofluidics, particle manipulation, and biology.[8−10] In general, the optical behavior of such dispersions is dictated by the features of the individual nanoparticles involved. This is particularly true in the case of metallic nanoparticles,[11−18] whose optical response is mediated by surface plasmon resonances[19,20] that can be readily tuned through composition, size, and shape.[20−24] Although the linear optical properties of these nanostructures have been extensively studied, much remains to be explored and understood in terms of their nonlinear characteristics. In this Letter we show that, by appropriately engineering the polarizability of plasmonic colloids, one can alter at will the associated nonlinear light−matter interactions in order to overcome the aforementioned challenges and hence to achieve deep beam penetration with suppressed diffraction.

As is well-known, the evolution of an optical beam propagating through a nanosuspension heavily depends on whether the polarizability of the constituent particles is positive (PP) or negative (NP). In the former case, the particles are attracted toward the regions of highest intensity, whereas in the latter they are expelled.[7,25] To first order, the underlying gradient force is given by $\vec{F}_{grad} = (1/4)\alpha_R \nabla|\vec{E}|^2$, where $\vec{E}$ is the electric field amplitude and α_R denotes the real part of the particle's polarizability.[26] Clearly, advances in locally manipulating particle concentrations within soft-matter systems are desired in a variety of settings, such as sorting different species, influencing osmotic effects, as well as locally initiating and controlling chemical reactions,[27] to name a few.

It is important to note that in both cases (PP and NP), the resulting local index change happens to be positive. The reason for this nonlinear, or intensity-dependent, effect is as follows. For PP particles, their index of refraction exceeds that of the background medium, and as a result the overall refractive index of the mixture locally increases. Conversely, the repulsion of NP particles (whose refractive index is below that of the background solvent) lowers their concentration, and therefore the effective index of refraction again increases along the path

Received: January 16, 2014
Revised: March 24, 2014
Published: April 3, 2014

   dx.doi.org/10.1021/nl500191e | *Nano Lett.* 2014, 14, 2498−2504

Table 1. Overview of the Four Exemplary Plasmonic Particle Geometries Investigated in This Work

#	1	2	3	4
Sample	Gold nanorods	Silica-gold core-shells	Gold spheres	Silver spheres
Parameters	50 nm, 100 nm	120 nm, 15 nm	40 nm	100 nm
Polarizablity at 532 nm	NP $\alpha_R < 0$	NP $\alpha_R < 0$	PP $\alpha_R > 0$	PP $\alpha_R > 0$

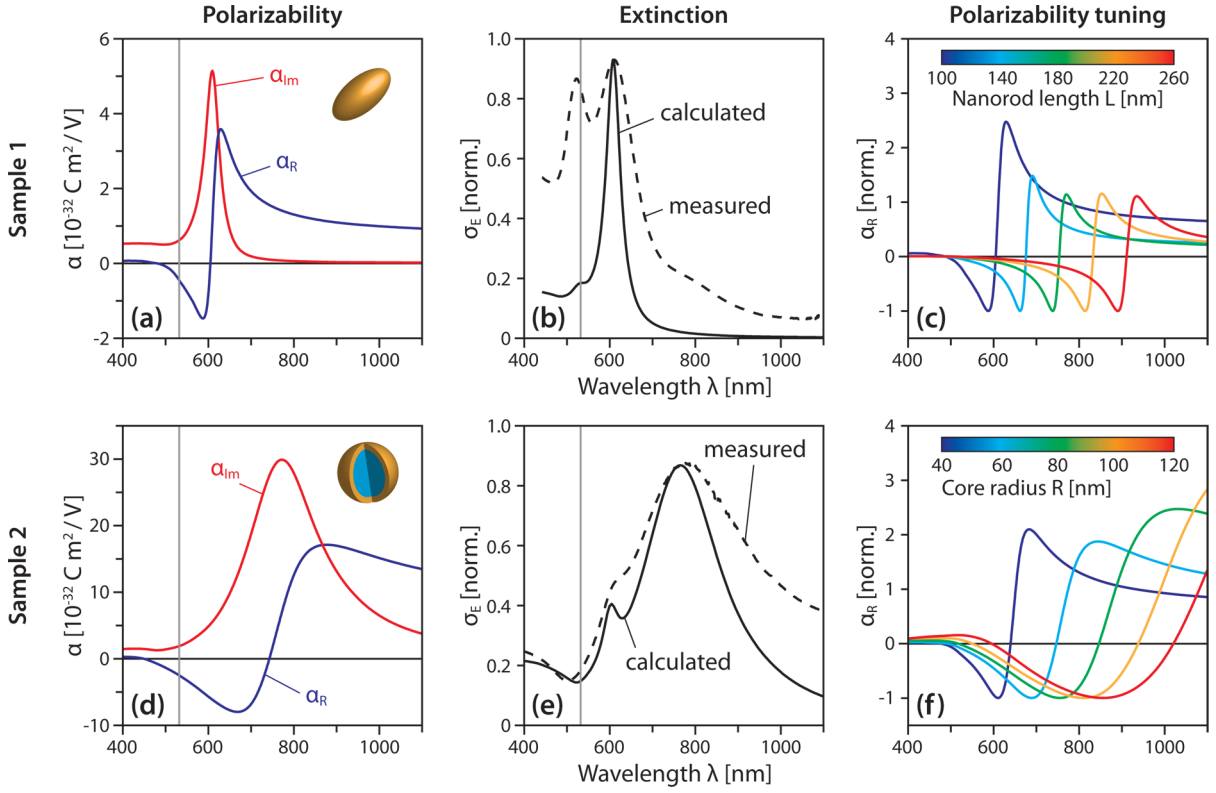

Figure 1. Calculated values for the polarizability of (a) gold nanorods (sample 1) and (d) silica–gold core–shell particles (sample 2) when suspended in water. Here, the blue and red curves represent the real part α_R and imaginary part α_{Im}, respectively. Both types of particles exhibit NP behavior at the experimental wavelength of 532 nm (indicated by vertical lines). The calculated and measured normalized extinction cross sections for samples 1 and 2 are displayed in (b) and (e), respectively. (c) Tunability of α_R for gold nanorods as a function of the rod length when the width is fixed at 50 nm. For reasons of visibility, all plots have been normalized. (f) Tuning of α_R for silica–gold core–shell particles similar to those in sample 2 as a function of the silica core size for a fixed shell thickness of 15 nm.

of the beam.[7] In both scenarios, this introduces a self-focusing nonlinearity capable of trapping an optical beam.[28,29] The interplay of wave propagation and particle concentration in such photoresponsive systems obeys a nonlinear Schrödinger-like equation[7]

$$i\frac{\partial\varphi}{\partial Z} + \frac{1}{2k_0 n_b}\nabla_\perp^2\varphi + k_0(n_p - n_b)\rho V\varphi + \frac{i\sigma\rho}{2}\varphi = 0 \quad (1)$$

where φ is the electric field envelope, $k_0 = (2\pi/\lambda_0)$ denotes the vacuum wavenumber, and σ is the Rayleigh scattering cross section.[30] V represents the volume of an individual particle and n_p its refractive index. Meanwhile, n_b stands for the refractive index of the background medium, and ρ denotes the intensity-dependent particle concentration. In this model, thermal effects have been neglected. The second term in eq 1 is responsible for diffraction effects, while the third and fourth terms account for a Kerr-type nonlinearity and scattering losses, respectively. As is well-known, systems governed by this class of equations in principle allow for two-dimensional self-trapped beams, or solitons. Yet, if the Kerr-nonlinearity is supercritical (i.e., the refractive index increases faster than linearly with intensity), beams inevitably tend to undergo catastrophic collapse. As was shown in previous studies based on a thermodynamic treatment of the ensemble, this is in fact the case for PP suspensions.[31] Apart from this intrinsic instability, the situation is further exacerbated by an equal increase in losses due to the attraction of scatterers to the beam, thereby further reducing the penetration depth.[32] If on the other hand a suspension is of NP type, the resulting nonlinearity turns out to be subcritical or saturable.[7] In this latter regime, these solitons, or "needles of light", are inherently stable and can propagate over several diffraction lengths without changing their shape. In addition, this is aided by a reduction of scattering losses as the NP

dx.doi.org/10.1021/nl500191e | Nano Lett. 2014, 14, 2498–2504

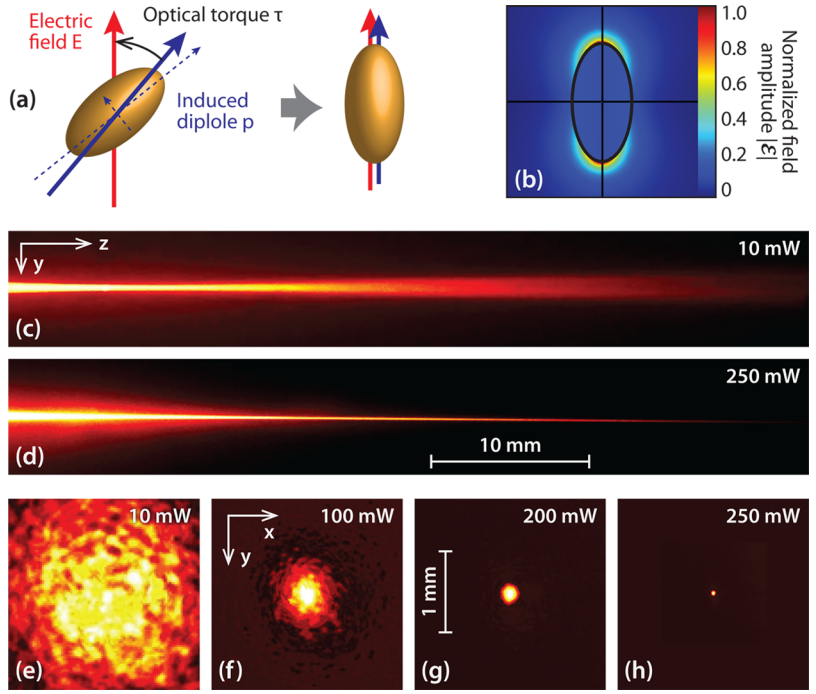

Figure 2. (a) Orientation of gold nanorods along the electric field $\vec{E}$ of a linearly polarized beam. (b) Field distribution around the nanorod at the longitudinal plasmon resonance. (c) Linear diffraction of a low-power beam (10 mW) when injected into an aqueous suspension of gold nanorods (sample 1). (d) Formation of a stable self-trapped filament at 250 mW over 5 cm (25 diffraction lengths) mediated by the negative polarizability of the colloid. (e–h) Beam profiles observed after 5 cm of propagation at different input power levels, showing the transition from diffractive broadening at 10 mW to self-trapping at 250 mW. For reasons of visibility, the output beam profiles have been normalized with respect to their individual peak intensities.

particle concentration is actively reduced along the beam path in an intensity-dependent fashion.

The polarizability of dielectric particles solely relies on their volume as well as the difference between their refractive index and that of the surrounding host medium. Note that the overwhelming majority of stable suspensions exhibit PP behavior, whereas dielectric NP dispersions are typically difficult to synthesize.[32] On the other hand, plasmonic resonances, which dominate the optical response of metallic nanoparticles, critically depend on their size, shape, and composition, as well as wavelength. As such, they offer a number of degrees of freedom in judiciously designing and fine-tuning their polarizability. In what follows, we will consider four exemplary plasmonic particle designs (see Table 1) with respect to their nonlinear behavior in colloidal suspensions and experimentally observe their impact on the propagation of intense laser beams. As we shall see, metallic nanosuspensions offer two fundamentally different mechanisms that enable light to overcome diffractive broadening as well as scattering losses, thus supporting stable self-trapped "needles of light". Interestingly, this is possible in both the NP and the PP regimes.

NP Plasmonic Nanosuspensions. While NP polarizabilities are difficult to obtain in dielectric realizations, they can be readily implemented in plasmonic settings. Even more importantly, plasmonic resonances can also be engineered to enhance the resulting polarizability values, in which case stable solitons can be observed at substantially lower power levels. Recent years have witnessed dramatic technological advances in both the design and the synthesis of plasmonic nanostructures. Here we investigate two types of such particles: gold nanorods (width 50 nm, length 100 nm, denoted as sample 1) and spherical core–shell particles (120 nm diameter silica core, 15 nm thick gold shell, denoted as sample 2). Figure 1 illustrates the resonant behavior of these two particle geometries. Whereas dielectric suspensions generally retain the sign of their polarizability over a broad range of wavelengths, the resonant nature of plasmonic structures leads to considerable variations of α_R, in both sign and amplitude, around a characteristic wavelength λ_r. Figure 1a shows this behavior for sample 1. While the real part of the polarizability is strongly positive above λ_r = 600 nm, a distinct NP region exists between 500 and 600 nm.

As a result, negative polarizabilities and repulsive forces can be expected up to about 550 nm, before losses associated with the imaginary part α_{Im} become relevant. In our calculations we assumed the principal axis of the nanorods to be oriented along the electric component $\vec{E}$ of the optical field. In a randomized setting, a summation of transverse and longitudinal resonances leads to an effective dipole moment $\vec{p}$. In the presence of a linearly polarized field, rods such as the ones considered here are known to orient themselves[33−35] along $\vec{E}$ following the optical torque $\vec{\tau} = \vec{p} \times \vec{E}$. In this alignment, the polarizability values are maximized, thereby enhancing the gradient force and in turn the local intensity-dependent refractive index change. Note that, by assuming this configuration, we neglect the influence of transverse resonances, as indicated by the single peak in the calculated extinction spectrum (solid line in Figure 1b). In contrast, the extinction measurements (dashed line) were carried out with unpolarized light and consequently exhibit an additional transverse resonance peak as well. The resonance wavelength λ_r can be freely tuned throughout the visible and near-IR region[19] by varying the particle geometry. Figure 1c shows the real parts of the calculated polarizability α_R

dx.doi.org/10.1021/nl500191e | Nano Lett. 2014, 14, 2498–2504

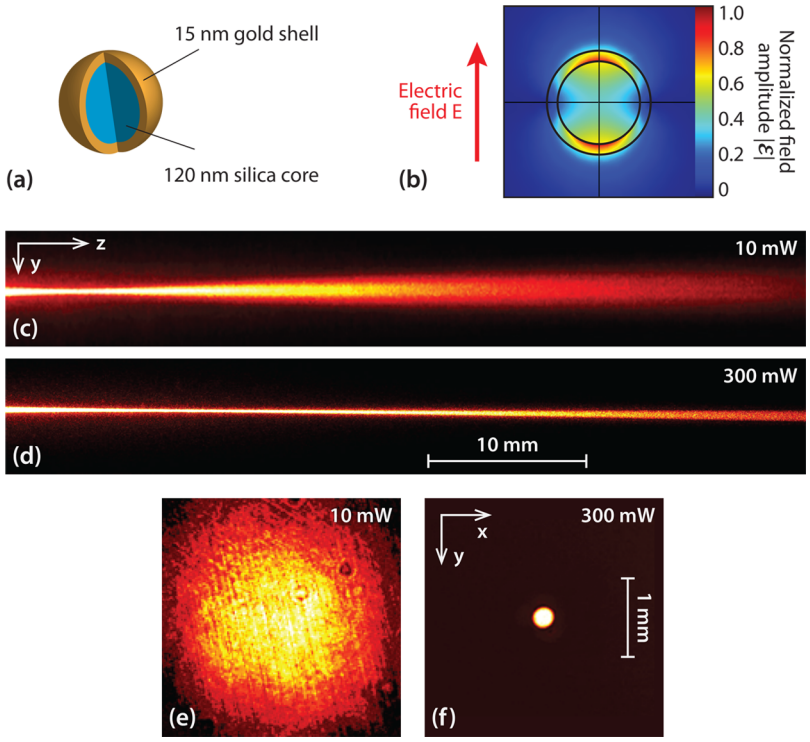

Figure 3. (a) Schematic of a silica–gold core–shell particle (sample 2) and (b) field distribution at its plasmon resonance. (c) Linear diffraction pattern at 10 mW and (d) stable soliton formation in the NP suspension at 300 mW. (e,f) Corresponding normalized output beam profiles after a propagation distance of 5 cm.

for different rod lengths ranging between 100 and 260 nm. As the nanorods become more elongated, the region of NP behavior shifts toward the infrared. On the other hand, a broader resonance and isotropic behavior can be achieved using spherically symmetric core–shell particles (sample 2, λ_r = 800 nm, see Figure 1d,e). Clearly, the system can be fine-tuned by modifying the ratio of core radius and shell thickness (see Figure 1f).

In order to verify the predicted behavior, we experimentally probed the nonlinear optical response of our nanoparticle dispersions. To this end, we observed the evolution of an initially focused continuous-wave laser beam (full width at half-maximum (fwhm) beam waist 15 μm, wavelength 532 nm, linearly polarized) through a 5 cm long glass cuvette filled with the respective colloids in aqueous suspensions. The respective volume filling fractions were chosen between f_V = (2, ..., 5) 10^{-6} to obtain samples of comparable optical density. The typical linear diffraction pattern obtained by exciting the nanorod dispersion (sample 1, Figure 2a,b) at a low power level (10 mW) is depicted in Figure 2c. At higher intensities, the nanorods are forced into alignment and subsequently expelled from the beam. As a result, the divergence gradually decreases until a sharply confined, needle-like optical filament emerges at a threshold power of $P_{th} \approx 250$ mW (Figure 2d). This self-trapped state is robust, as illustrated by the absence of diffraction or beam collapse over the whole sample length of 5 cm. Figures 2e–h show the transition from linear diffraction broadening to a stable soliton as observed at the end face of the cuvette. Similar results have been obtained for the core–shell particles of sample 2 (see Figure 3). The major difference between the two suspensions is the 5-fold larger negative polarizability in the latter (core–shell) sample as compared to that in previous (nanorod) one. By virtue of the proportionally larger gradient force, core–shell particles are repelled much more efficiently, resulting in an up to three times wider self-trapped beam at powers comparable to P_{th} in sample 1. We would like to emphasize that the negative polarizability values obtained in our plasmonic settings are at least an order of magnitude larger than those encountered in typical dielectric NP nanoparticles. This is also evidenced by the stable propagation over more than 25 diffraction lengths, compared to only a few diffraction lengths in dielectric suspensions.[32] Likewise, plasmonically mediated localization occurs for powers in the range of a few hundred milliwatts, as opposed to several watts in dielectric settings with otherwise comparable parameters.[32,36]

PP Plasmonic Nanosuspensions. As mentioned earlier, plasmonic structures may exhibit not only NP behavior but also substantially higher positive polarizabilities around the resonance wavelength. In line with the findings in dielectric PP suspensions, one might therefore expect that such enhanced supercritical nonlinearities would cause a catastrophic self-focusing beam collapse even at low powers. Surprisingly, several independent reports on the nonlinear response in noble-metal nanocolloids[37−39] have indicated a defocusing Kerr response. The question naturally arises as to how these apparently contradictory results can be reconciled and how PP plasmonic suspensions do actually interact with an intense laser beam. To this end, we again consider two types of particles: gold spheres (diameter 40 nm, denoted as sample 3) and slightly larger silver spheres (diameter 100 nm, denoted as sample 4). Figure 4a,d shows plots of the wavelength-dependent complex polarizability. Both structures clearly exhibit PP characteristics at the probe wavelength 532 nm, whereas the real part α_R of the polarizability of the silver spheres exceeds that of the smaller gold spheres by about an order of magnitude. The resulting

dx.doi.org/10.1021/nl500191e | Nano Lett. 2014, 14, 2498−2504

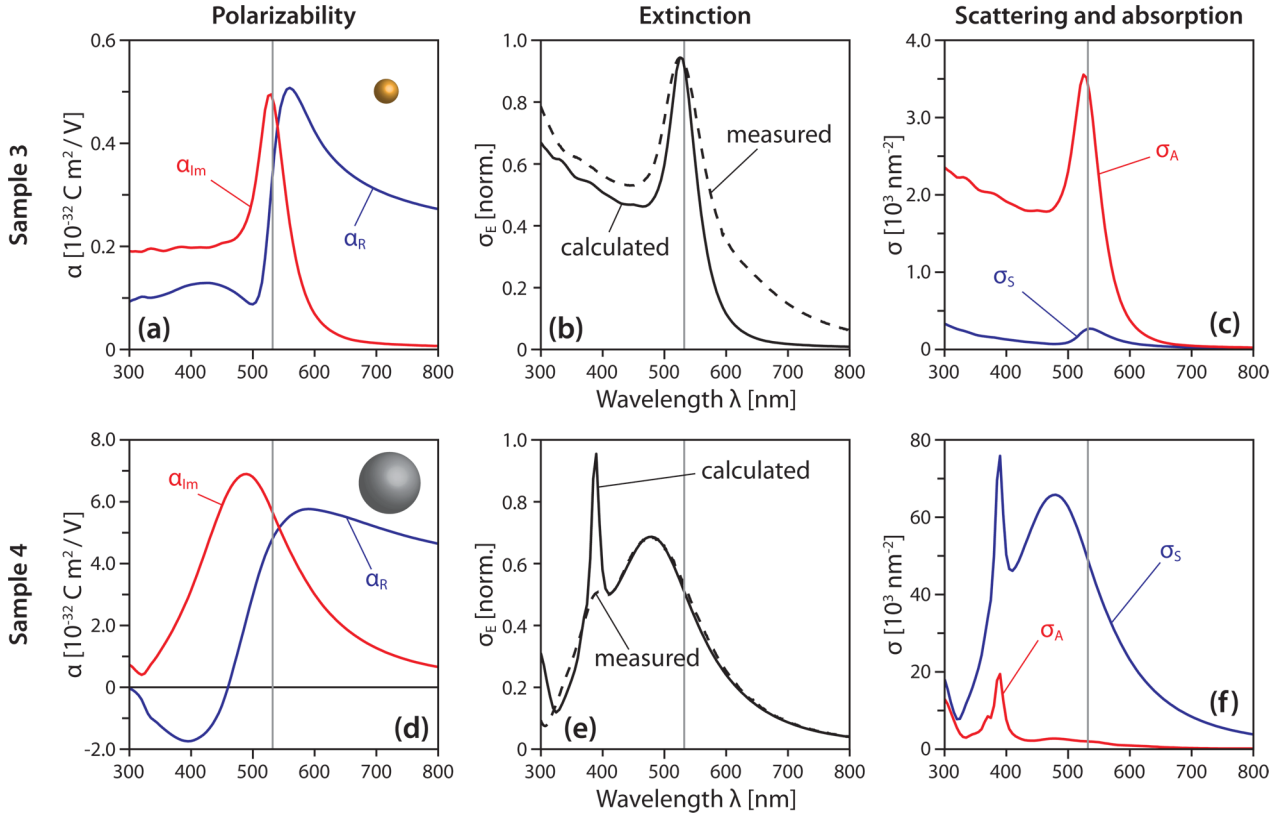

Figure 4. Calculated values for the polarizability of (a) gold spheres (diameter 40 nm, sample 3) and (d) silver spheres (diameter 100 nm, sample 4) when suspended in water. Here, the blue and red curves represent the real part α_R and imaginary part α_{Im}, respectively. Both types of particles exhibit PP behavior at the experimental wavelength of 532 nm indicated by vertical lines. The calculated and measured normalized extinction cross sections for samples 3 and 4 are displayed in (b) and (e), respectively. (c,f) Calculated absorption- and scattering cross sections σ_A and σ_S of the gold and silver spheres, respectively. Note that for sample 3, absorption is the dominant effect ($\sigma_A \gg \sigma_S$), while in sample 4 scattering plays the major role ($\sigma_A \ll \sigma_S$) at 532 nm.

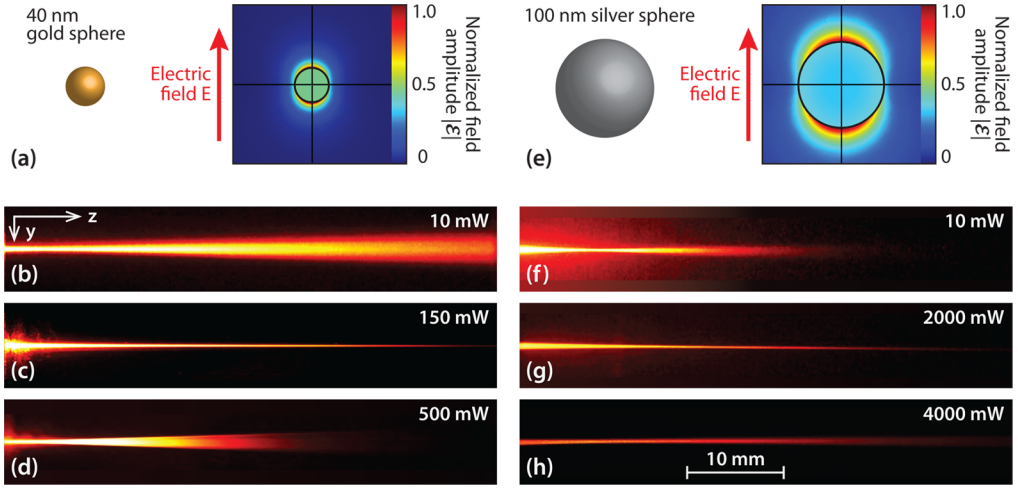

Figure 5. Field distributions at the plasmon resonances of (a) 40 nm gold spheres (sample 3) and (b) 100 nm silver spheres (sample 4), respectively. Sample 3: (b) Linear diffraction at 10 mW, (c) thermally mediated stable self-trapping under PP conditions at 150 mW, and (d) thermal nonlinear defocusing at 500 mW. Sample 4: (f) Catastrophic collapse in the PP suspension at 10 mW. (g) Around 2000 mW, thermal effects become strong enough to balance the supercritical PP nonlinearity and stabilize the beam. (h) Thermal defocusing eventually overcomes the self-focusing process.

theoretical extinction cross sections are compared to the measured values in Figure 4b,e. Notably, throughout the visible spectrum the gold particles primarily exhibit absorption ($\sigma_A \gg \sigma_S$), while scattering dominates the overall extinction of the silver spheres ($\sigma_A \ll \sigma_S$) (see Figure 4c,f). Figure 5 depicts the experimentally observed propagation patterns in these two nanoplasmonic PP suspensions. Interestingly, light injected into sample 3 (gold spheres, Figure 5a) exhibits self-trapping and stable soliton propagation over the entire length of the cuvette as the power reaches 150 mW (Figure 5b,c). Given the positive polarizability, at this point one may ask what mechanism prevents the self-focusing collapse. Intuition might suggest an

dx.doi.org/10.1021/nl500191e | Nano Lett. 2014, 14, 2498−2504

eventual saturation of the nonlinearity due to osmotic pressure effects.[40] Yet, such particle interactions are not specific to metallic structures, and moreover, one would require an extreme increase in particle concentration to compensate for the supercritical response in the dilute suspensions considered in our experiments. As it turns out, absorption is the decisive factor: The probe wavelength happens to coincide with sample 3's surface plasmon resonance at 543 nm. Consequently, individual particles convert a large fraction of the incident light to thermal energy instead of scattering it. This heat is quickly transferred to the surrounding liquid and, in accordance with the negative thermooptic coefficient of water,[41] lowers the background refractive index n_b. While in the NP regime thermal effects play a minor role (given that the particles are expelled from the beam), in the PP case the particle displacement actually serves to enhance them. Mathematically, the thermal defocusing response can be incorporated into eq 1 as follows:

$$i\frac{\partial}{\partial Z}\varphi + \frac{1}{2k_0 n_b}\nabla_\perp^2\varphi + k_0(n_p - n_b)\rho V\varphi - k_0|\Delta n_T|\varphi + \frac{i\sigma\rho}{2}\varphi = 0 \quad (2)$$

In this equation, Δn_T denotes the thermally mediated refractive index change of the suspension and can be approximated by $\Delta n_T = (\partial n_b/\partial T)(T - T_b)(1 - f_V)$, where T represents the spatial temperature distribution and T_b is the initial temperature of the suspension. In our system, the thermooptic coefficient is negative: $\partial n_b/\partial T \approx -10^{-4}$ K^{-1}. As we can see, the interplay between the focusing colloidal nonlinearity (third term in eq 2) and the self-defocusing thermal behavior (fourth term in eq 2) yields an overall response akin to that of a cubic-quintic saturable nonlinear medium. Indeed, as the power is further increased, nonlinear defocusing dominates, and the beam diverges strongly (Figure 5d). This behavior is consistent with the previously reported negative Kerr coefficients.[37,38] The experimental results obtained with sample 4 further corroborate this hypothesis. At 532 nm, the polarizability α_R of the silver spheres (Figure 5e) amounts to about 15× that of the smaller gold particles, while their absorption is significantly lower. As a result, the gradient forces are of sufficient strength to collapse the beam even at powers as low as 10 mW (Figure 5f), while thermal effects are minimal. As the particle accumulation saturates, the defocusing thermal nonlinearity slowly gains traction and eventually becomes strong enough to stabilize the beam at about 2 W (Figure 5g). Above 4 W, self-defocusing becomes dominant, and the beam diverges again (Figure 5h).

In summary, we have demonstrated that plasmonic nanoparticles provide a versatile platform for controlling the flow of light in soft-matter systems. The resonant nature of the light–matter interaction provides new degrees of freedom in terms of engineering the sign and value of the resulting polarizability. As a result, we observed for the first time self-trapping and robust soliton propagation of light over distances up to 25 diffraction lengths, which would have been otherwise impossible in conventional dielectric settings. Our findings may open up new opportunities in synthesizing novel soft-matter media with tailored optical nonlinearities. By dramatically increasing the depth of penetration in colloidal systems, these results could be useful in deploying highly efficient spectroscopic techniques such as SERS[42] in settings, which are otherwise inaccessible due to scattering.

AUTHOR INFORMATION

Corresponding Authors

*E-mail: demetri@creol.ucf.edu.

*E-mail: zhigang@sfsu.edu.

Notes

The authors declare no competing financial interest.

ACKNOWLEDGMENTS

This work was supported by the Air Force Office of Scientific Research (MURI grants FA9550-10-1-0561, FA9550-12-1-0148, FA9550-12-1-0111, FA9550-13-1-0024), and by NSF (grants ECCS-1128520, PHY-1100842). M.H. was supported by the German National Academy of Sciences Leopoldina (grant LPDS 2012-01). The authors would like to thank Dr. Andrew Ichimura at SFSU for his assistance.

REFERENCES

(1) Smith, P. W.; Maloney, P. J.; Ashkin, A. *Opt. Lett.* **1982**, *7*, 347–349.

(2) Vlassopoulos, D.; Fytas, G. From Polymers to Colloids: Engineering the Dynamic Properties of Hairy Particles. In *High Solid Dispersions*; Cloitre, M., Ed.; Springer-Verlag: Berlin, 2010; Vol. *236*, pp 1–54.

(3) Jones, R. A. L. *Soft Condensed Matter*; Oxford University Press: New York, NY, 2002.

(4) Yethiraj, A.; van Blaaderen, A. *Nature* **2003**, *421* (6922), 513–517.

(5) Liu, A. J.; Nagel, S. R. *Nature* **1998**, *396* (6706), 21–22.

(6) Marburger, J. H. *Prog. Quantum Electron.* **1975**, *4*, 35–110.

(7) El-Ganainy, R.; Christodoulides, D. N.; Rotschild, C.; Segev, M. *Opt. Express* **2007**, *15*, 10207–10218.

(8) Lee, S. K.; Kim, S. H.; Kang, J. H.; Park, S. G.; Jung, W. J.; Yi, G. R.; Yang, S. M. *Microfluid. Nanofluid.* **2008**, *4*, 129–144.

(9) Jonáš, A.; Zemánek, P. *Electrophoresis* **2008**, *29*, 4813–4851.

(10) Glatter, O. *Prog. Colloid Polym. Sci.* **1991**, *84*, 46–54.

(11) Lal, S.; Link, S.; Halas, N. J. *Nat. Photonics* **2007**, *1*, 641–648.

(12) Oldenburg, S. J.; Averitt, R. D.; Westcott, S. L.; Halas, N. J. *Chem. Phys. Lett.* **1998**, *288*, 243–247.

(13) Anker, J. N.; Hall, W. P.; Lyandres, O.; Shah, N. C.; Zhao, J.; Van Duyne, R. P. *Nat. Mater.* **2008**, *7*, 442–453.

(14) Rosi, N. L.; Mirkin, C. A. *Chem. Rev.* **2005**, *105*, 1547–1562.

(15) Jain, P. K.; Huang, X. H.; El-Sayed, I. H.; El-Sayed, M. A. *Acc. Chem. Res.* **2008**, *41*, 1578–1586.

(16) Willets, K. A.; Van Duyne, R. P. *Annu. Rev. Phys. Chem.* **2007**, *58*, 267–297.

(17) Daniel, M. C.; Astruc, D. *Chem. Rev.* **2004**, *104*, 293–346.

(18) Argyropoulos, C.; Chen, P. Y.; Monticone, F.; D'Aguanno, G.; Alù, A. *Phys. Rev. Lett.* **2012**, *108*, 263905.

(19) Bohren, C. F.; Huffman, D. R. *Absorption and Scattering of Light by Small Particles*; Wiley: New York, 1983.

(20) Kelly, K. L.; Coronado, E.; Zhao, L. L.; Schatz, G. C. *J. Phys. Chem. B* **2003**, *107*, 668–677.

(21) Link, S.; El-Sayed, M. A. *J. Phys. Chem. B* **1999**, *103*, 4212–4217.

(22) Noguez, C. *J. Phys. Chem. C* **2007**, *111*, 3806–3819.

(23) Alù, A.; Engheta, N. *J. Appl. Phys.* **2005**, *97*, 094310.

(24) Prodan, E.; Nordlander, P. *J. Chem. Phys.* **2004**, *120*, 5444–5454.

(25) Ashkin, A. *Phys. Rev. Lett.* **1970**, *24*, 156–159.

(26) Salandrino, A.; Fardad, S.; Christodoulides, D. N. *J. Opt. Soc. Am. B* **2012**, *29*, 855–866.

(27) Adleman, J. R.; Boyd, D. A.; Goodwin, D. G.; Psaltis, D. *Nano Lett.* **2009**, *9*, 4417–4423.

(28) Chen, Z.; Segev, M.; Christodoulides, D. N. *Rep. Prog. Phys.* **2012**, *75*, 086401.

(29) Lamhot, Y.; Barak, A.; Peleg, O.; Segev, M. *Phys. Rev. Lett.* **2010**, *105*, 163906.

(30) van de Hulst, H. C. *Light Scattering by Small Particles*; Dover Publication, Inc.: New York, 1981.
(31) El-Ganainy, R.; Christodoulides, D. N.; Wright, E. M.; Lee, W. M.; Dholakia, K. *Phys. Rev. A* **2009**, *80*, 053805.
(32) Man, W. N.; Fardad, S.; Zhang, Z.; Prakash, J.; Lau, M.; Zhang, P.; Heinrich, M.; Christodoulides, D. N.; Chen, Z. G. *Phys. Rev. Lett.* **2013**, *111*, 218302.
(33) Selhuber-Unkel, C.; Zins, I.; Schubert, O.; Sonnichsen, C.; Oddershede, L. B. *Nano Lett.* **2008**, *8*, 2998−3003.
(34) Pelton, M.; Liu, M. Z.; Kim, H. Y.; Smith, G.; Guyot-Sionnest, P.; Scherer, N. E. *Opt. Lett.* **2006**, *31*, 2075−2077.
(35) Bonin, K. D.; Kourmanov, B.; Walker, T. G. *Opt. Express* **2002**, *10*, 984−989.
(36) Fardad, S.; Mills, M. S.; Zhang, P.; Man, W. N.; Chen, Z. G.; Christodoulides, D. N. *Opt. Lett.* **2013**, *38*, 3585−3587.
(37) Jia, T. J.; He, T. C.; Li, P. W.; Mo, Y. J.; Cui, Y. T. *Opt. Laser Technol.* **2008**, *40*, 936−940.
(38) Karimzadeh, R.; Mansour, N. *Opt. Laser Technol.* **2010**, *42*, 783−789.
(39) Souza, R. F.; Alencar, M.; da Silva, E. C.; Meneghetti, M. R.; Hickmann, J. M. *Appl. Phys. Lett.* **2008**, *92*, 201902.
(40) Lee, W. M.; El-Ganainy, R.; Christodoulides, D. N.; Dholakia, K.; Wright, E. M. *Opt. Express* **2009**, *17*, 10277−10289.
(41) Schiebener, P.; Straub, J.; Sengers, J.; Gallagher, J. S. *J. Phys. Chem. Ref. Data* **1990**, *19*, 677−717.
(42) Bell, S. E. J.; McCourt, M. R. *Phys. Chem. Chem. Phys.* **2009**, *11*, 7455−7462.